MOLECULAR IMAGING AND BIOLOGY

Published Online: 30 November 2011

Mol Imaging Biol (2012) 14:637–646
DOI: 10.1007/s11307-011-0527-x

RESEARCH ARTICLE

^{99m}Tc-labeled Rituximab for Imaging B Lymphocyte Infiltration in Inflammatory Autoimmune Disease Patients

G. Malviya,[1,2] K. L. Anzola,[3] E. Podestà,[4] B. Laganà,[4] C. Del Mastro,[1] R. A. Dierckx,[2] F. Scopinaro,[1] A. Signore[1,2]

[1]*Nuclear Medicine Department, Faculty of Medicine and Surgery, "Sapienza" University of Rome, Via di Grottarossa 1035, 00189 Rome, Italy*

[2]*Department of Nuclear Medicine and Molecular Imaging, University Medical Centre Groningen, University of Groningen, Groningen, The Netherlands*

[3]*Nuclear Medicine Unit, Clinica Colsanitas, Bogotà, Colombia*

[4]*Allergy, Clinical Immunology and Rheumatology Unit, Faculty of Medicine and Surgery, "Sapienza" University of Rome, Rome, Italy*

Abstract

Purpose: The rationale of the present study was to radiolabel rituximab with 99m-technetium and to image B lymphocytes infiltration in the affected tissues of patients with chronic inflammatory autoimmune diseases, in particular, the candidates to be treated with unlabelled rituximab, in order to provide a rationale for 'evidence-based' therapy.

Procedures: Rituximab was labelled with ^{99m}Tc via 2-ME reduction method. *In vitro* quality controls of ^{99m}Tc-rituximab included stability assay, cysteine challenge, SDS-PAGE, immunoreactive fraction assay and competitive binding assay on CD20+ve Burkitt lymphoma-derived cells. For the human pilot study, 350–370 MBq (100 μg) of ^{99m}Tc-rituximab were injected in 20 patients with different chronic inflammatory autoimmune diseases. Whole body anteroposterior planar scintigraphic images were acquired 6 and 20 h p.i.

Results: Rituximab was labelled to a high labelling efficiency (>98%) and specific activity (3515–3700 MBq/mg) with retained biochemical integrity, stability and biological activity. Scintigraphy with ^{99m}Tc-rituximab in patients showed a rapid and persistent spleen uptake, and the kidney appeared to be a prominent source for the excretion of radioactivity. Inflamed joints showed a variable degree of uptake at 6 h p.i. in patients with rheumatoid arthritis indicating patient variability; similarly, the salivary and lacrimal glands showed variable uptake in patients with Sjögren's syndrome, Behçet's disease and sarcoidosis. Inflammatory disease with particular characteristics showed specific uptake in inflammatory lesions, such as, dermatopolymyositis patients showed moderate to high skin uptake, a sarcoidosis patient showed moderate lung uptake, a Behçet's disease patient showed high oral mucosa uptake and a polychondritis patient showed moderate uptake in neck cartilages. In one patient with systemic lupus erythematosus, we did not find any non-physiological uptake.

Conclusion: Rituximab can be efficiently labelled with ^{99m}Tc with high labelling efficiency. The results suggest that this technique might be used to assess B lymphocyte infiltration in affected organs in patients with autoimmune diseases; this may provide a rationale for anti-CD20 therapies.

Key words: Rituximab, Anti-CD20 antibody, Radiolabelling, Molecular imaging, Therapy decision making

Correspondence to: G. Malviya; *e-mail:* gaurav.malviya@yahoo.com

Introduction

Rheumatoid arthritis (RA), psoriatic arthritis (PsA), Sjögren's syndrome (SS), systemic lupus erythematosus (SLE), dermatopolymyositis, Behçet's disease, sarcoidosis and polychondritis are chronic inflammatory autoimmune diseases, and their treatment is often complicated. It has been shown that targeting B cells can directly alter autoimmune responses [1] in patients with these diseases. In the last few decades, our knowledge about the crucial role of B lymphocytes in disease pathogenesis has been increased from the advancement made in the understanding of human immune system, including mechanisms of lymphocyte activation and antigen processing, immune tolerance, T and B lymphocytes crosstalk, and the role of pro-inflammatory cytokines in autoimmune processes [2–6]. B cells are responsible for the production of auto-antibodies and rheumatoid factor and are also involved in T cell activation, pro-inflammatory cytokine production and therefore play an important role in the pathogenesis of inflammatory autoimmune diseases [7, 8]. These cells have been found in pathological infiltrates in affected tissues of patients with autoimmune diseases and are implicated in disease progression [9]. The development of mature B cells from stem cells involves several stages, each of which changes in expression of a wide range of cell surface markers. Thus, there are several potential candidates, on which B cell-depleting therapies can act directly, via use of monoclonal antibody (mAb) directed against cell surface markers (such as CD19, CD20, CD22) [10, 11] or indirectly via blockade of cytokine pathways (such as TNF-α, interleukin-6, B lymphocyte stimulator (BLyS) and proliferation-inducing ligand APRIL) [12]. CD20 is expressed on more than 95% of B lymphocyte from blood and lymphoid organs, therefore particularly suitable target for immunotherapy [7]. This antigen expressed on the surface of B cell precursors, mature B cells and B cell lymphomas, but is not expressed on hemopoietic stem cells, pro-B cells, normal plasma cells, dendritic cells and other normal tissues. Anti-CD20 therapies include the humanized anti-CD20 mAbs ocrelizumab and veltuzumab, and the fully human mAb ofatumumab. These antibodies vary in the extent of humanization and have different complement dependent cytotoxicity (CDC), and antibody-dependent cell-mediated cellular cytotoxicity (ADCC). Recently, TRU-015, a new anti-CD20 small modular immunopharmaceutical protein (SMIP) has been engineered, which is a dimeric, single-chain polypeptide (approximately one third to one half the size of mAb), for the treatment of RA and lymphoma [13, 14].

Rituximab (MabThera®; F. Hoffmann-La Roche Ltd., Switzerland/Rituxan®; Biogen IDEC Pharmaceuticals Inc., USA), is an IgG1κ isotype chimeric anti-CD20 mAb that binds specifically to the transmembrane CD20 antigen. Rituximab was the first chimeric mAb approved by the United States Food and Drug Administration in 1997 for the treatment of malignancy, and in 2006 for the treatment of patients with active RA, who do not respond to one or more tumor necrosis factor (TNF) antagonist therapies. Rituximab promote B cell lysis by CDC, ADCC and induction of apoptosis.

The above data highlighted the opportunity to use the radiolabelled anti-CD20 mAb probe for *in vivo* imaging of CD20 positive B lymphocyte infiltration in inflammatory lesions. Such a probe would also allow non-invasive evaluation of disease extent and severity in patients affected by autoimmune diseases thus allowing better staging of the disease, since this might be difficult to assess by other conventional techniques [15]. This approach, moreover, may allow to perform an 'evidence-based biological therapy' with a view to assessing whether the antibody will localize in an inflammatory foci before using the same unlabelled anti-CD20 for therapy. Since, biological therapies are expensive and can be associated with severe side effects, scintigraphy with radiolabelled rituximab might prove particularly important for the selection of patients to be treated with unlabelled rituximab and may also be useful in patient follow-up for monitoring the efficacy of therapy.

Materials and Methods

Antibody

Rituximab (MabThera®) was provided by F. Hoffmann-La Roche Ltd., Switzerland.

Labelling of Rituximab with 99m-Technetium

Rituximab was labelled with 99m-technetium using a direct, 2-mercapthoethanol (2-ME) reduction method, as previously described [16]. Briefly, disulfide bridges of the mAb were reduced by incubating a molar excess of 2-ME with rituximab solution (Mabthera®), for 30 min at room temperature in the dark. Different molar ratios between 2-ME: mAb (1,000:1, 2,000:1 and 4,000:1) were used in order to achieve the best activation of antibody and consequently the highest labelling efficiency (LE). Before labelling, activated antibody was purified by G-25 Sephadex PD10 desalting columns (GE Healthcare) and N_2 purged cold phosphate buffer saline (pH 7.4) as eluant. After activation and purification, the antibody was aliquoted in 100 µg each vial, and stored at −80°C, up to their use for radiolabelling.

Methylene diphosphonic acid (MDP) was used as weak transchelating ligand. The bone scan kit (Osteocis®, CIS Bio International) containing 3 mg methylene diphosphonic acid, 0.45 mg $SnCl_2.2H_2O$, 0.75 mg of ascorbic acid, 10.0 mg of sodium chloride was reconstituted with 1 ml of N_2 purged normal saline solution. Different amounts (from 1 to 10 µl) of methylene-diposphonate solution were tested with 100 µg of activated antibody and 370 MBq of $^{99m}TcO_4^-$ freshly eluted from a $^{99}Mo/^{99m}Tc$ generator in order to achieve the highest LE. In the preparation of the radiopharmaceutical, all clinical grade reagents were used under sterile conditions.

Radiochemical Purity

Quality controls were performed using Instant Thin Layer Chromatography-Silica Gel (ITLC-SG) strips (VWR International). The strips were analyzed on a radio-scanner (Bioscan Inc.) to quantitate the percentage of activity bound to the mAb. When 0.9% NaCl was used as the solvent (with normal ITLC-SG strips), retention factors (R*f*) were: ^{99m}Tc-rituximab=0.0; ^{99m}Tc-MDP and free $^{99m}TcO_4^-$= 0.9–1.0, whereas elution of albumin absorbed ITLC-SG strips with NH_3/H_2O/ethanol (1:5:2) resulted in R*f* values of: ^{99m}Tc-colloids= 0.0; ^{99m}Tc-rituximab, and free $^{99m}TcO_4^-$=0.9–1.0.

Stability

Stability of ^{99m}Tc-rituximab in human serum and normal saline was measured up to 22 hours, in four replicates. One milliliter of fresh human serum was added, in each of four aliquots of radiolabelled rituximab (100 µg) and incubated at 37°C. In another four aliquots of radiolabelled rituximab (100 µg), 1 ml of normal saline was added in each, was added and incubated at room temperature. The percentage of free $^{99m}TcO_4^-$ and radioactivity bound to mAb were measured at different time points (1, 3, 6 and 22 h) by ITLC-SG (as described above).

A cysteine challenge assay was also performed to check the *in vitro* stability of radiolabelled antibody at 37°C for 60 min, in four replicates. ^{99m}Tc-rituximab was incubated at different molar ratios of cysteine and mAb, ranging from 64:1 at the highest cysteine concentration to zero in the absence of cysteine. At the end of the incubation time, each reaction mixture was evaluated by ITLC-SG, as described above. All known chemical forms of ^{99m}Tc-cysteine have *Rf* values between 0.5 and 1.0, when normal saline is used as a eluent.

Structural Integrity

Possible modifications induced by 2-ME reduction procedure on rituximab were tested by sodium dodecyl sulphate-polyacrylamide gel electrophoresis (SDS-PAGE) in non-reducing conditions. Equal amount of protein (Native mAb, activated mAb and radiolabelled mAb) in each lane (25 µg) were subjected to 8% SDS-PAGE, at 45 mA constant voltage, along with protein molecular weight marker (11–250 kD, BioRad). After 2 h of electrophoresis, the gel was stained with Coomassie brilliant blue G250 (Sigma-Aldrich) for 60 min and washed thrice (15 min each) with a methanol/H_2O/acetic acid (4.5:4.5:1) solution.

Autoradiography of ^{99m}Tc-rituximab was also performed to check the incorporation of radioactivity in mAb after radiolabelling. For this purpose, radiolabelled mAb (11.1 MBq) was loaded in a separate lane of SDS-PAGE. The gel was exposed to a Kodak® BioMax photographic plate (Sigma-Aldrich) for 20 min, and the photographic plate was developed subsequently by using Kodak® GBX developer/replenisher (Sigma-Aldrich) and Kodak® GBX fixer/replenisher (Sigma-Aldrich) solutions, according to standard procedure.

Sterility

Radiolabelled mAb was sterilized by filtration through 0.22 µm Millipore GV syringe filter (low protein-binding filter) into a sterile vial, under the aseptic condition. Sterility test was performed on single-patient doses from three different batches, by direct inoculation method using heamoculture vials, Plus+Anarobic/F and Plus+Arobic/F (BD BACTEC™, BD Biosciences); these vials were incubated at 37°C for 7 days.

In vitro competitive binding assay

To test the *in vitro* binding ability of ^{99m}Tc-labelled rituximab with specific receptors, a competitive binding assay was performed on CD20 positive, Burkitt lymphoma-derived cell line, RAJI [17]. The cell were maintained in an RPMI 1640 culture medium (Sigma-Aldrich) supplemented with 10% heat inactivated foetal calf serum (Gibco), 1% L-glutamine (Gibco), 1% antibiotics (penicillin and streptomycin, Gibco), at 37°C in a 5% CO_2 humidified incubator. Cell viability and cell count was determined by trypan blue assay using a haemocytometer.

For binding experiment, ^{99m}Tc-rituximab at increasing concentrations (from 0.05 to 50 nM) were incubated in triplicate with 4×10^5 cells alone or in the presence of 100 molar excess of the unlabelled antibody to saturate the specific receptor on cells. After 2 h of incubation, cells harvested by centrifugation (9,000×*g* for 3 min) and washed two times with complete RPMI 1640 culture medium. Cells and supernatants were collected in different vials and were counted separately for radioactivity in a single-well gamma counter (Gammatom s.p.a., Italy). The curve of specific binding was generated as difference between total binding and non-specific binding. A Scatchard analysis was performed by using GraphPad Prism Version 5.00 Software (GraphPad Software, Inc.) to determine the dissociation constant (Kd).

Immunoreactive Fraction Assay

The assay for determination of the fraction of immunoreactive antibody by linear extrapolation to conditions representing infinite antigen excess has been adapted with slight modifications from the method described by Lindmo et al. [18].

The immunoreactive fraction assay was performed using a constant concentration of radiolabelled mAb and serial dilutions of RAJI cells. The cells were washed three times in phosphate-buffered saline (pH 7.4) and suspended in a cold phosphate-buffered saline (PBS) with 1% bovine serum albumin (BSA) solution. Radiolabelled mAb at a constant concentration of 50 ng/ml, in PBS with 1% BSA solution was added to different amounts of cells (final concentration ranging from 2.6×10^6 to 0.08×10^6 cells/ml). Cells were incubated for 2 h at 4°C and then washed twice with 500 µl of cold PBS with 1% BSA solution, before counting cell-associated radioactivity in a single-well gamma counter. The data were plotted as a double inverse plot of the applied radiolabelled antibody over the specific binding as a function of the inverse cell concentration. In this plot, the origin of the abscissa represents infinite cell concentration, i.e., conditions of infinite antigen excess. All experiments were performed in duplicate.

Patients

We studied 20 consecutive patients (M/F, 4/16; mean age, 55.5± 11.65 years; mean disease duration, 12±99.3 months) who met with our inclusion criteria (stated below) and referred to the outpatient clinic of the rheumatology unit of 'Sapienza' University

of Rome (Italy) due to chronic inflammatory autoimmune diseases, including RA, PsA, dermatopolymyositis, sarcoidosis, Sjögren's syndrome, SLE, Behçet's disease and polychondritis (n=5, 3, 5, 2, 2, 1, 1 and 1, respectively). All patients agreed to participate in the study and signed a written informed consent. None of the enrolled patient received unlabelled rituximab therapy before the study.

Inclusion criteria for patients were different depending on the type of pathology. RA: a moderate/high disease activity evaluated by a disease activity score (DAS) on 44 joints >3.7 [19], despite a treatment with disease-modifying anti-rheumatic drugs (DMARDs), including methotrexate at adequate dose and the failure of at least one TNF-α-blocker drug; all RA patients were candidates for a second level therapy as an anti-CD20 monoclonal antibody. PsA: a moderate/high disease activity evaluated by the swollen and tender joints count, patient and physician global assessment, despite a treatment with DMARDs and TNF-α blockers. Dermatopolymyositis: patients with an insufficient response to corticosteroids to commonly used immunosuppressants (azathioprine, mycophenolate, methotrexate or cyclosporine) or to high dose i.v. immunoglobulins, documented by clinical evaluation and altered laboratory tests. Sarcoidosis: a resistant disease to steroids, immunosuppressive drugs and/or antimalarial therapies. Sjögren's syndrome: an active disease, resistant to substitute agents for sicca features, glucocorticoids and immunosuppressive agents for extra-glandular involvement. SLE: a moderate/severe disease activity evaluated by the systemic lupus erythematosus disease activity index (SLEDAI) [20] despite standard doses of steroid and immunosuppressive therapy. Behçet's disease: an active disease, resistant to standard treatment including immunosuppressive agents such as azathioprine and cyclosporine in combination with corticosteroids and colchicine. Polychondritis: a poorly controlled disease, despite non-steroidal anti-inflammatory drugs, immunosuppressants (particularly methotrexate) or steroids.

Clinical assessment

Patients were evaluated by the same rheumatologist, and data were collected into a standardized case record forms, which included demographics, diagnosis, date of diagnosis, comorbidities, past and present treatments, biological therapies if prescribed, the start of the treatment and concomitant medications. Diagnosis of all mentioned diseases (RA, PsA, dermatopolymyositis, sarcoidosis, Sjögren's syndrome, SLE, Behçet's disease and polychondritis) were formulated according to international classification criteria for each illness [21–28].

Non-specific and specific laboratory tests, including erythrocyte sedimentation rate (ESR), C-reactive protein (CRP), muscle enzymes, immunological analysis such as Anti-nuclear antibodies (ANA), extractable nuclear antigens (ENA) profile, rheumatoid factor, anti-citrullinated peptide antibodies and human leukocyte antigen (HLA)-B51 detection (only for Behçet's patient) were performed. When necessary, patients underwent other imaging procedures, such as chest radiography, computed tomography (CT) of chest, functional pulmonary tests and bronchoalveolar lavage (BAL) for sarcoidosis; ostheo-articular ultrasonography (US) or magnetic resonance imaging (MRI) for RA and PsA; salivary glands US for Sjögren's syndrome; and muscles MRI for dermatopolymyositis .

Clinical evaluation in arthritis (RA and PsA) patients included count of swollen and tender joints, patient and physician global assessment (visual analog scale, VAS). Overall disease activity was also measured for RA patients with the DAS 44 which takes in consideration pain and swollen in 44 joints.

A biopsy for tissues of interest, such as dermal, muscular and salivary gland was performed in dermatopolymyositis and Sjögren's syndrome patients.

Scintigraphic Studies with ^{99m}Tc-Rituximab

All patients underwent immunoscintigraphy, before treatment with unlabelled rituximab, to assess uptake of ^{99m}Tc-rituximab in the inflammatory lesions. Anterior planar whole body images were acquired 6 and 20 hours after i.v. administration of 350–370 MBq (100 µg) of ^{99m}Tc-rituximab. Planar anterior and posterior images of affected sites were also acquired at 6 and 20 hours. Images were acquired with a Philips Sky-Light dual head gamma camera fitted with a high resolution collimator. Whole body planar images were acquired on 256×1024 pixel matrix at 10 cm/min (at 6 h) or 5 cm/min (at 20 h) scanning speed. "Static regional images" were acquired on 512 x 512 pixel matrix for 300 seconds (at 6 h) or 600 seconds (at 20 h). A time-mode, rather than a count-mode acquisition modality was chosen to be able to compare images of different patients, being injected with almost the same dose of radioactivity, thus avoiding operator bias in image acquisition and analysis.

The scintigraphic scans were interpreted by two experienced nuclear medicine physicians. The interpreters had clinical information obtained from the patient's referring physician but no information on the other imaging modality. Nevertheless, the uptake interpretation were describe as mild, moderate and high comparing with the heart and large blood vessel activity. An uptake was considered as 'mild' when it was lower than heart and large blood vessel uptake, 'moderate' when it was equal to heart and large blood vessel uptake, and 'high' when it was higher than heart and large blood vessel uptake.

Statistical analysis

The student t-test was used to compare quantitative variables in the same group. A p value less than 0.05 was considered statistically significant.

Results

Radiochemical Purity

By using a direct labelling method, the best results were obtained when disulfide bridges of the antibody were reduced using a 2,000-fold excess of 2-ME. An increase in 2-ME concentration for reduction of rituximab, results in decreased LE, and higher colloid percentage. We obtained a high LE (>98%) with negligible amount of colloids (<2%) with high specific activity (3,515–3,700 MBq/mg), when the activated mAb was labelled with ^{99m}Tc by using only 3 µl of methylene diphosphonic acid solution (from the bone scan kit). Thus, a post labelling purification step could be avoided.

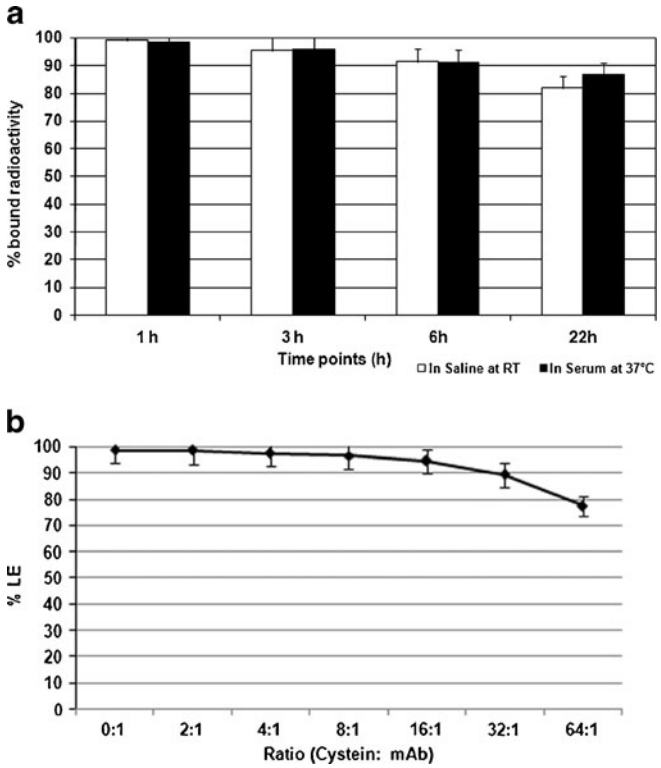

Fig. 1. **a** Stability of ^{99m}Tc-rituximab in saline and in plasma assessed by ITLC-SG at different time points. **b** Cysteine challenge assay of ^{99m}Tc-rituximab assessed by ITLC-SG at increasing ratio between cysteine to mAb.

Stability

Radiolabelled rituximab was stable when incubated in fresh human serum or in normal saline up to 22 h, as shown in Fig. 1a. After 22 h, still more than 80% of the radioactivity was bound to the antibody in both media. The results of cysteine challenge assay also demonstrated that radiolabelled rituximab was stable, approximately 95% intact when exposed to up to a 16-fold excess of cysteine (Fig. 1b).

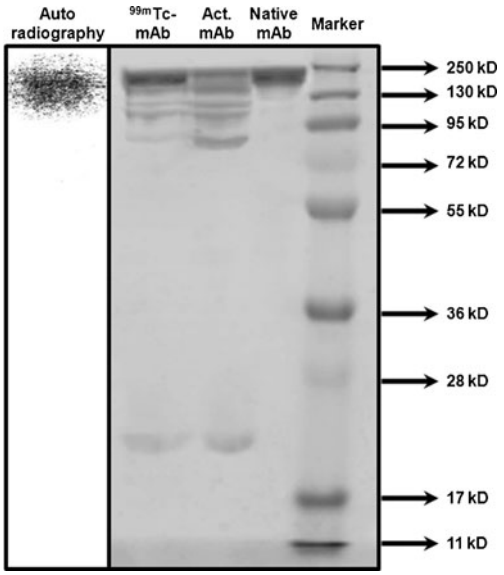

Fig. 2. SDS-PAGE analysis performed in non-reducing condition showing native, activated and ^{99m}Tc labelled rituximab lane. The autoradiography analysis (*first lane*) showing radioactivity associated with the band of complete mAb (145 kDa).

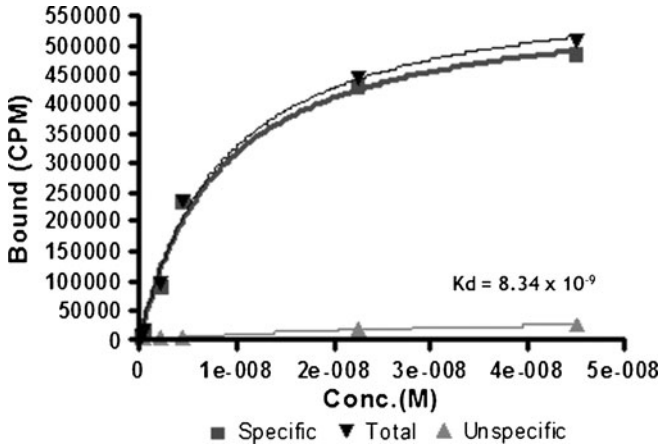

Fig. 3. Saturation binding curve of ^{99m}Tc-labelled rituximab to RAJI cells. Kd for ^{99m}Tc-rituximab 8.3 nM. Curve fitting was performed using GraphPad software.

Structural Integrity

SDS-PAGE analysis of native, activated and radiolabelled rituximab show, one thick band of 145 kilodalton (kDa) in native rituximab lane; bands of different molecular weights in activated rituximab lane probably due to light/heavy chain complexes after 2-ME reduction; whereas, mainly one thick band of approximately 145 kDa in radiolabelled rituximab lane, i.e., the molecular weight of intact mAb (Fig. 2). Autoradiography of ^{99m}Tc-rituximab lane, showed that almost all radioactivity was attached with the band of higher molecular weight (145 kDa).

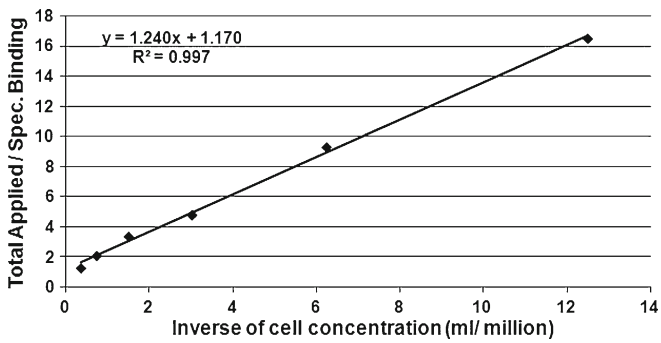

Fig. 4. A double inverse plot of the immunoreactivity fraction assay was used to determine immunoreactive fraction (i.e., 85.5%).

Table 1. Clinical and scintigraphic findings of patients

Disease	No. of patients	Sex	Age (years)	Diseaseduration (years)	^{99m}Tc-anti-CD20 mAb scintigraphy uptake at 6 h							
					Affected joints	Lung	Salivary glands	Lacrimal glands	Skin	Cartilages	Buccal mucosa	Spleen
Rheumatoid arthritis	5	5 F	58±14.9	12.6±14.6	+/+++	−/+	−	−	−	+/+++	−	+++
VAS (mean±SD): 75±11.2 DAS 44 (mean±SD): 4.9±1.1		ESR (mm/h) (mean±SD): 29±22 Swelling: knees, ankles, shoulders, wrists							CRP (mean±SD): 0.55±13.4 Tenderness: knees, ankles, shoulders, wrists			
Psoriatic arthritis	3	1 M, 2 F	45.7±12.5	2.33±3.2	+/+++	−/+	−	−	−	+/+++	−	+++
ESR (mm/h) (mean±SD): 35±31 Tenderness: knees, ankles, shoulders, wrists		CRP (mean±SD): 0.8±2.2							Swelling: knees, ankles, shoulders, wrists			
Dermatopolymyositis	5	1 M, 4 F	58.8±5.9	5.4±5.6	−	−	−	−	+/+++	−	−	+/+++
ESR (mm/h) (mean±SD): 29±18		CRP (mean±SD): 0.5±0.1							Dermal biopsy: +ve			
Sjögren syndrome	2	2 F	80, 66	1, 0.5	−/++	−/+	+/+++	++	−	−	−/+	+++
US: +ve salivary glands Salivary gland biopsy: +ve		ESR (mm/h) (mean±SD): 17, 19							CRP (m ean±SD): 1.1, 0.7			
Sarcoidosis	2	1 M, 1 F	48, 58	1, 1	−/+	+/++	++/+++	+/++	−	−	−	+++
ESR (mm/h): 34, 19		CRP (mean±SD): 0.4, 0.25							BAL: +ve			
Systemic lupus erythematosus	1	F	41	0.5	−	+	−	−	−	−	−	+++
ESR (mm/h): 69		CRP: 0.44										
Behçet's disease	1	M	51	1	+	−	+++	++	−	−	+++	+++
ESR (mm/h): 3		CRP: 0.4							Swelling: two ankles			
Tenderness: left ankle, lombalgia		Oral aphtosis										
Polychondritis ESR (mm/h): 15	1	F CRP: 0.1	54	3	−	−	+	−	−	++	−	+++

VAS visual analogue scale, *ESR* erythrocyte sedimentation rate, *CRP* C-reactive protein, *DAS 44* disease activity score, *US score* ultrasonography score. (+, mild uptake; ++, moderate uptake; +++, high uptake; −, no detectable uptake of the radiopharmaceutical over background).

Sterility

The sterility test did not show any Gram+ve or –ve bacterial growth in heamoculture vials inoculated with ^{99m}Tc labelled rituximab.

In vitro competitive binding assay

The saturation binding curve was plotted as a specific bound radioactivity against increasing molar concentration of radiolabelled mAb showed a plateau (Fig. 3). A 100-fold molar excess of unlabelled antibody saturates the receptors present on cells, and consequently prevented the specific binding of the radiolabelled rituximab, which shows that rituximab retained its specific binding activity with CD20 receptors expressed on RAJI cells, even after the radiolabelling with technetium-99 m. Kd for ^{99m}Tc-rituximab 8.3 nM, which is only slightly higher than the Kd of native rituximab, i.e., 5.2 nM.

Immunoreactive Fraction Assay

The data demonstrate a very close linear relationship of 'total applied/ specific binding' as a function of the inverse cell concentration. Fitting of a straight line to the data by means of linear regression analysis allows an easy and precise determination of the intercept value at the ordinate. This value equals 1/immunoreactive fraction; thus in this case, the immunoreactive fraction was 85.5%, as indicated in the Fig. 4.

Clinical Assessment

In clinical evaluation, all RA patients had moderate pain, and swelling and/or tenderness in knees and wrists, ankles, shoulders. VAS was 75±11.2, ESR was 29±22, CRP was 0.55±13.4, DAS 44 was 4.9±1.1. PsA patients had a mean ESR of 35±31 and CRP of 0.8±2.2; they also showed moderate pain and swelling and/or tenderness in the knees, wrists, ankles and shoulders.

The ESR (millimeters per hour) and CRP (milligrammes per liter) values, evaluated before the scan of patients with dermatopolymyositis, Sjögren's syndrome, sarcoidosis, SLE, Behçet's disease and polychondritis are shown in Table 1. Additionally, patients with dermatopolymyositis and Sjögren's syndrome had positive biopsies, and both Sjögren's syndrome patients were reported positive for ultrasonography (US) of the salivary glands. Moreover, both sarcoidosis patients had a positive BAL, and an oral aphtosis was noticed in Behçet's disease patient confirming the disease.

Scintigraphic Studies with ^{99m}Tc-Rituximab

After i.v. administration of ^{99m}Tc-rituximab (350–370 MBq; 100 μg), the whole body images were acquired at 6 and 20 h. We observed a mild to moderate to high uptake in the

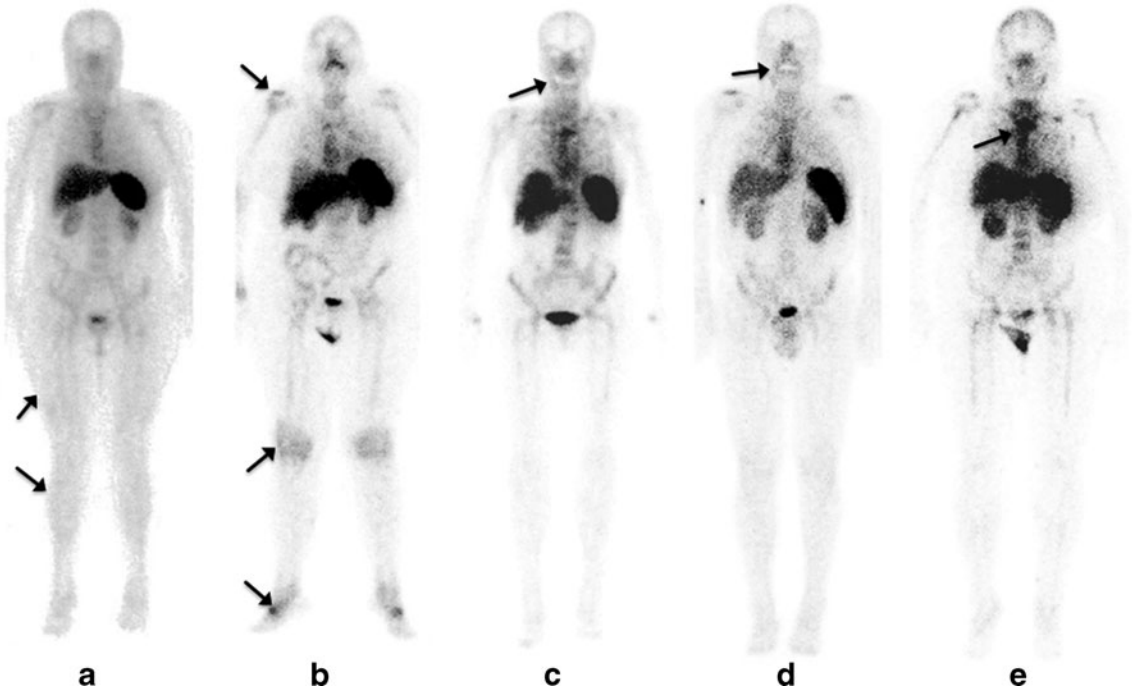

Fig. 5. Whole body scintigraphic images at 6 h with ^{99m}Tc-rituximab in patients with **a** dermatopolymyositis (see skin uptake). **b** Rheumatoid arthritis (see joint uptake). **c** Sjögren's syndrome (see salivary and lacrimal gland uptake). **d** Behçet's disease (see oral mucosa uptake). **e** Sarcoidosis (see lung uptake).

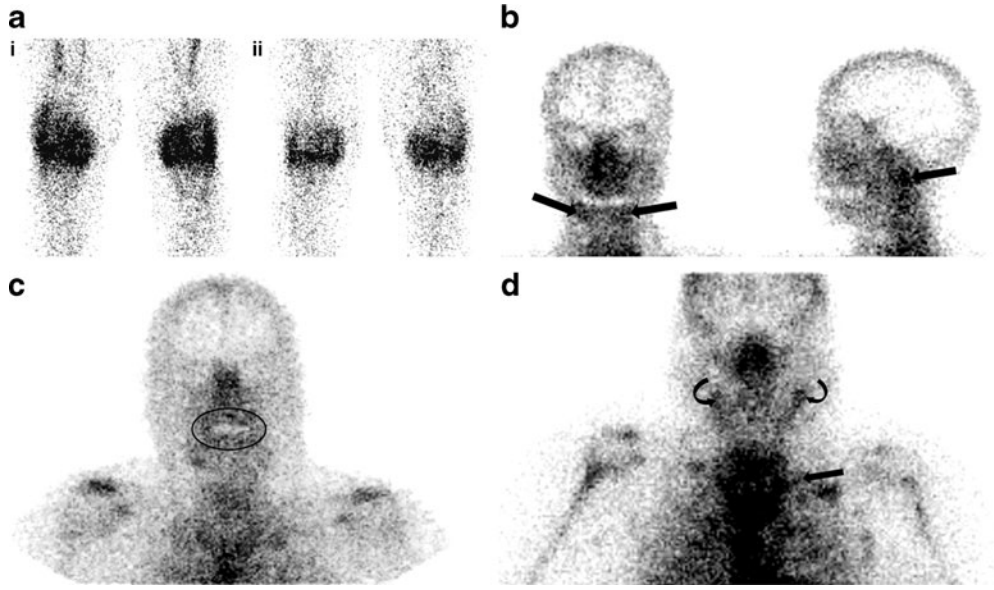

Fig. 6. Static regional scintigraphic images with ^{99m}Tc-rituximab in patients with **a** Rheumatoid arthritis (at *i* 6 h and *ii* 20 h). **b** Sjögren's syndrome (at 6 h). **c** Behçet's disease (at 6 h). **d** Sarcoidosis (at 6 h).

affected regions at 6 h p.i., in all the patients with different autoimmune diseases (Fig. 5a–e and Table 1). At 20 h, we found a low background activity and consequently higher target to background (T/B) ratio.

In the five patients with active RA and the three patients with PsA, we observed an uptake of the radiopharmaceutical in the known affected joints (including knees, wrists, elbows, phalanges, ankles and shoulders). This uptake was variable and not every patient did show uptake in each clinically affected joint(s) (Fig. 6a).

Muscle and skin uptake in patients with dermatopolymyositis were detected; however, this kind of scintigraphy was more positive at 20 h when the background blood pool activity was decreased. Interestingly, in one dermatopolymyositis patient we found a very mild spleen uptake, in contrast to the high uptake normally present in all other subjects. After that, FACS analysis of peripheral blood cells confirmed the presence of a significantly low B lymphocyte count in this patient.

Patients suffering from Sjögren's disease showed a variable ^{99m}Tc-rituximab uptake in salivary and moderate uptake lachrymal glands (Fig. 6b).

Scintigraphy in the patient with Behçet's disease demonstrated clearly detectable buccal ^{99m}Tc-rituximab activity at 6 h p.i. (Fig. 6c).

We also performed scintigraphic examination in one patient with sarcoidosis in which a mild ^{99m}Tc-rituximab uptake was found in the nasal cavity, salivary and lachrymal glands (Fig. 6d) similar to the so-called "Panda Sign" described for scintigraphy with ^{67}Ga-citrate [29]. However, we could not see a high uptake in the lung region, as per our expectation.

An SLE patient was difficult to evaluate. We found a mild radiopharmaceutical uptake in the lung region. This patient did not show uptake in clinically defined inflammatory lesions.

The patient with polychondritis showed an abnormal radiopharmaceutical uptake in the cartilages of the neck (thyroid and cricoid cartilages) and in a regional lymph node. Some faint uptake was also detectable in the submandibular salivary glands.

A variable thyroid uptake was detected in ten out of 20 patients (50%). We therefore wanted to investigate whether there was an autoimmune reaction in these patients and we asked them to test anti-thyroglobulin (anti-Tg) and anti-thyroid peroxidase antibody (anti-TPO). Interestingly, five of these patients showed increased anti-thyroid auto-antibodies, whereas amongst the ten patients without thyroid uptake of ^{99m}Tc-rituximab, none had increased anti-thyroid auto-antibodies.

None of the patients showed any kind of side effect, adverse event or other type of reaction following the administration of the radiotracer used, either immediately after injection or after 1 month.

Discussion

Previous studies with radiolabelled non-specific probes (such as ^{99m}Tc-human polyclonal immunoglobulins, ^{67}Ga-citrate, ^{99m}Tc-albumin nanocolloids, ^{18}F-FDG, ^{99m}Tc- and ^{111}In- labelled liposomes) were focused on the detection of the state of activity of the disease [30, 31]. Nevertheless, no real clinical advantages have been proved comparing this radiopharmaceuticals to other available diagnostic techniques (such as ultrasonography, X-ray, magnetic resonance imaging) with regard to the clinical management of patients. The real breakthrough in targeted immunoscintigraphy for inflammatory disease patients is the possibility to highlight the presence of the relevant receptors involved in the pathophysiology of the disease directly by means of the

specific radiolabelled mAbs that will eventually be used for treatment. Some radiolabelled mAbs (such as anti-E-selectin and anti-CD4) demonstrated their excellent capability for the localization of inflammatory regions, but lack of their use for the therapeutic purposes, thus limiting their further development and use for immunoscintigraphy. However, approval of mAbs for therapeutic purposes (such as anti-CD20 for treatment of rheumatic patients) provides us an opportunity to select the patients through this technique.

In the present study, we aimed to radiolabel rituximab with ^{99m}Tc for scintigraphic studies, and then, as a proof of concept, we evaluated its *in vivo* localisation pattern in a cohort of patients affected by different autoimmune diseases. The results obtained so far are highly encouraging and hold promise for therapy decision making and follow-up, with a view to assessing whether an antibody will accumulate in an inflamed tissue before using the same unlabelled antibody for therapeutic purposes. This kind of information can only be obtained with such kind of imaging approach based on new radiopharmaceuticals that provide a solid basis for the further development and clinical use of immunoscintigraphy in inflammatory autoimmune disease patients.

We demonstrated that rituximab could be labelled with ^{99m}Tc without any modification in its biological activity and specificity for CD20 receptors *in vivo*. Direct radiolabelling method using 2-ME reduction of antibody, is simple, rapid, reliable and yielding high LE with excellent *in vivo* targeting. We always labelled antibody to a high labelling efficiency (>98%) and specific activity (3,515–3,700 MBq/mg). SDS-PAGE and autoradiography analysis demonstrated that the radioactivity stands with whole antibody molecule (band of 145 kD). Our immunoreactive fraction assay demonstrated that 85.5% of the antibody was immunoreactive even after the radiolabelling procedure.

For scintigraphic studies, we injected a tracer dose of 350–370 MBq (100 μg) of rituximab, which is a much lower dose in comparison with therapeutic dose (with no adverse or allergic reaction) that is unlikely to alter the natural history of the disease or have any therapeutical effect.

In patients, at 6-h images, ^{99m}Tc-rituximab was detectable in the heart and large vessels, liver, spleen and kidneys with more variable uptake in the lungs, thyroid and bone marrow. Rapid and persistent uptake of the spleen was also concordant with results recently published by Stopar et al. in patients with B cell non-Hodgkin's lymphoma [32]. At 20-h images, we observed reduction of blood pool activity and lung activity with increased liver and spleen activity. Bowel activity was never detected. Thyroid and salivary gland uptake was not always concordant, and stomach uptake was never detected. Thyroid uptake could be correlated to the presence of subclinical autoimmune phenomena in this organ, since the presence of anti-thyroid auto-antibodies in five out of ten patients with thyroid uptake. In the remaining five patients (with thyroid uptake but without anti-thyroid auto-antibodies) we cannot exclude the presence of a "silent" lymphocyte infiltration as well as possible uptake of free Tc, the latter possibility being, however, unlikely because of the absence of salivary gland uptake in these patients.

The use of radiolabelled mAbs against lymphocyte antigens for therapy decision making was already exlplored by us with success and clinical benefit. The most clinically relevant example is the immunoscintigraphy with ^{99m}Tc-anti-TNF-α mAb in Crohn's disease (CD) and RA patients [16, 33]. In the first study in CD patients, ^{99m}Tc-infliximab (a commercially available mAb anti-TNF-α) showed uptake in the affected bowel only in few patients that responded to anti-TNF treatment [16]. In another study in patients with active RA before intra-articular treatment with infliximab, we observed a variable degree of joint uptake that did not correlate with swelling or pain of the joint, but could predict the success of therapy [33]. These studies demonstrated that radiolabelled anti-TNF-α scintigraphy could be useful for improving the selection of those patients who could benefit most from therapy with TNF-α antagonists, an example of the use of immunoscintigraphy for therapy decision making. In line with this strategy, in the present study, scintigraphic images with ^{99m}Tc-rituximab demonstrated moderate to high accumulation in some affected joints of arthritis patients, but some other swelling and painful joints were negative at the scan. This suggests that not all joints have a similar pattern of B lymphocyte infiltration and, therefore, the total-body evaluation of CD20 positivity should be mandatory before initiating anti-CD20 therapy. Overall, our data demonstrated different biodistribution of radiolabelled CD20 in different patients, thus different degrees of B lymphocyte infiltration in different tissues of different patients. Our results are encouraging and hold promise not only for imaging of B lymphocyte infiltration in inflammatory diseases but, most importantly, for mapping B lymphocytes in affected tissues of each patient in order to establish a personalized therapy.

Despite large prospective studies being required to confirm the clinical utility of this technique in each disease, data obtained so far indicate that the information about the presence of drug targets for personalised therapy, by means of immunoscintigrapy, is of great clinical and social relevance for optimizing treatments, avoiding unnecessary therapies and reducing costs thus providing a cost-effective solution for biological therapies.

Conflict of Interest Disclosure. The authors declare that they have no conflict of interest.

References

1. Hiepe F, Radbruch A (2005) B cells in autoimmunity: more than antibodies? Blood 106(7):2227
2. Mitchison NA, Wedderburn LR (2000) B cells in autoimmunity. Proc Natl Acad Sci USA 97:8750–8751
3. Gause A, Berek C (2001) The role of B cells in the pathogenesis of rheumatoid arthritis. Potential implications for treatment. BioDrugs 15:73–79

4. Takemura S, Klimiuk PA, Braun A, Goronzy JJ, Weyand CM (2001) T cell activation in rheumatoid synovium is B cell dependent. J Immunol 167:4710–4718
5. Zhang Z, Bridges SL (2001) Pathogenesis of rheumatoid arthritis. Role of B-lymphocytes. Rheum Dis Clin North Am 27:335–353
6. Dörner T, Burmester GR (2003) The role of B cells in rheumatoid arthritis: mechanisms and therapeutic targets. Curr Opin Rheumatol 15:246–252
7. Stashenko P, Nadler LM, Hardy R, Schlossman SF (1980) Characterization of a human B-lymphocyte-specific antigen. J Immunol 125:1678–1685
8. Tedder TF, Boyd AW, Freedman AS, Nadler LM, Schlossman SF (1985) The B cell surface molecule B1 is functionally linked with B-cell activation and differentiation. J Immunol 135(2):973–979
9. Teng YK, Levarht EW, Hashemi M, Bajema IM, Toes RE, Huizinga TW, van Laar JM (2007) Immunohistochemical analysis as a means to predict responsiveness to rituximab treatment. Arthritis Rheum 56:3909–3918
10. De Vita S, Zaja F, Sacco S, De Candia A, Fanin R, Ferraccioli G (2002) Efficacy of selective B cell blockade in the treatment of rheumatoid arthritis, evidence for a pathogenetic role of B cells. Arthritis Rheum 46 (8):2029–2033
11. Malviya G, Galli F, Sonni I, Pacilio M, Signore A (2010) Targeting T and B lymphocytes with radiolabelled antibodies for diagnostic and therapeutic applications. Q J Nucl Med Mol Imaging 54(6):654–676
12. Dörner T, Kinnman N, Tak PP (2010) Targeting B cells in immune-mediated inflammatory disease: a comprehensive review of mechanisms of action and identification of biomarkers. Pharmacol Ther 125:464–475
13. Burge DJ, Bookbinder SA, Kivitz A, Fleischmann RM, Shu C, Bannink J (2008) Pharmacokinetic and pharmacodynamic properties of TRU-015, a CE20-directed small modular immunopharmaceutical protein therapeutic, in patients with rheumatoid arthritis: a phase I, open-label, dose-escalation clinical study. Clin Ther 30:1806–1816
14. Stromatt S, Chopiak V, Dvoretskiy L et al (2009) Sustained safety and efficacy of TRU-015 with continued retreatment of rheumatoid arthritis subjects following a phase 2B study [abstract 403]. Arthritis Rheum 60 (suppl 10):S148–S149
15. Malviya G, Conti F, Chianelli M, Scopinaro F, Dierckx RA, Signore A (2010) Molecular imaging of rheumatoid arthritis by radiolabelled monoclonal antibodies: new imaging strategies to guide molecular therapies. Eur J Nucl Med Mol Imaging 37(2):386–398
16. D'Alessandria C, Malviya G, Viscido A, Aratari A, Maccioni F, Amato A, Scopinaro F, Caprilli R, Signore A (2007) Use of a 99 m-technetium labelled anti-TNF-α monoclonal antibody in Crohn's Disease: *in vitro* and *in vivo* studies. Q J Nucl Med Mol Imaging 51:1–9
17. Schaffland AO, Buchegger F, Kosinski M, Antonescu C, Paschoud C, Grannavel C, Pellikka R, Delaloye AB (2004) ^{131}I-rituximab: relationship between immunoreactivity and specific activity. J Nucl Med 45:1784–1790
18. Lindmo T, Boven E, Cuttitta F, Fedorko J, Bunn PA Jr (1984) Determination of the immunoreactive fraction of radiolabelled monoclonal antibodies by linear extrapolation to binding at infinite antigen excess. J Immunol Methods 72:77–89
19. Fransen J, van Riel PLCM (2005) The disease activity score and the EULAR response criteria. Clin Exp Rheumatol 23:S93–S99
20. Bombardier C, Gladman DD, Urowitz MB, Caron D, Chang CH (1992) Derivation of the SLEDAI. A disease activity index for lupus patients. The Committee on Prognosis Studies in SLE. Arthritis Rheum 35:630–640
21. Arnett FC, Edworthy SM, Bloch DA et al (1988) The American Rheumatism Association 1987 revised criteria for the classification of rheumatoid arthritis. Arthritis Rheum 31(3):315–324
22. Taylor W, Gladman D, Helliwell P, Marchesoni A, Mease P, Mielants H (2006) CASPAR Study Group. Classification criteria for psoriatic arthritis: development of new criteria from a large international study. Arthritis Rheum 54:2665–2673
23. Dalakas MC (1991) Polymyositis, dermatomyositis and inclusion body myositis. N Engl J Med 325:1487–1498
24. Ryu JH, Daniels CE, Hartman TE, Yi ES (2007) Diagnosis of interstitial lung diseases. Mayo Clin Proc 82(8):976–986
25. Vitali C, Bombardieri S, Jonsson R et al (2002) Classification criteria for Sjögren's syndrome: a revised version of the European criteria proposed by the American–European Consensus Group. Ann Rheum Dis 61(6):554–558
26. Tan EM, Cohen AS, Fries JF, Masi AT, McShane DJ, Rothfield NF et al (1982) The 1982 revised criteria for the classification of systemic lupus erythematosus. Arthritis Rheum 25:1271–1277
27. International Study Group for Behcet's Disease (ISGBD) (1990) Criteria for diagnosis of Behcet's disease. Lancet 335:1078–1080
28. McAdam LP, O'Hanlan MA, Bluestone R, Pearson CM (1976) Relapsing polychondritis: prospective study of 23 patients and a review of the literature. Medicine 55:193–215
29. Kurdziel KA (2000) The panda sign. Radiology 215:884–885
30. Chianelli M, D'Alessandria C, Conti F, Valesini G, Annovazzi A, Signore A (2006) New radiopharmaceuticals for imaging rheumatoid arthritis. Q J Nucl Med Mol Imaging 50(3):217–225
31. Signore A, Mather SJ, Piaggio G, Priori R, Malviya G, Dierckx RA (2010) Molecular imaging of inflammation/infection: nuclear medicine and optical imaging agents and methods. Chem Rev 110(5):3112–3145
32. Gmeiner Stopar T, Fettich J, Zver S, Mlinaric-Rascan I, Hojker S, Socan A, Peitl PK, Mather S (2008) 99mTc-labelled rituximab, a new non-Hodgkin's lymphoma imaging agent: first clinical experience. Nucl Med Commun 29(12):1059–1065
33. Malviya G, D'Alessandria C, Lanzolla T, Lenza A, Conti F, Valesini G, Scopinaro F, Dierckx RA, Signore A (2008) 99 m-Technetium labelled anti-TNFα antibodies for the therapy decision making and follow-up of patients with rheumatoid arthritis. Q J Nucl Med Mol Imaging; 52 Suppl 1(2):13